

Dynamic curve type serves as an effective tool for the diagnosis of benign or malignant non-mass enhancements on breast MRI

TARA FAROOQ KAREEM¹, AREEGE MUSTAFA KAMAL² and MUNAWAR AL NAKASH¹

¹Department of Surgery, College of Medicine, University of Baghdad, Baghdad 89WG+GX, Iraq;

²Department of Pathology, Oncology Teaching Hospital, Medical City, Baghdad 89WH+9MF, Iraq

Received July 9, 2025; Accepted January 12, 2026

DOI: 10.3892/ol.2026.15567

Abstract. Identifying malignant non-mass enhancement (NME) in contrast-enhanced breast magnetic resonance imaging (MRI) remains a notable diagnostic challenge due to overlapping imaging features between benign and malignant lesions. Although the delayed-phase kinetic patterns are well-established, the diagnostic value of the initial-phase kinetics has not been fully elucidated. The present study aimed to evaluate the dynamic and morphological characteristics of NME lesions, to determine whether incorporating initial-phase kinetics with delayed-phase analysis improves the discrimination between benign and malignant cases. A prospective study was conducted at the Oncology Teaching Hospital (Baghdad, Iraq) from April to December 2022, including patients referred for breast MRI. Only cases with pure NME (without associated mass lesions) were included. A core biopsy was performed for all cases, with excisional biopsy when indicated. Data collection followed the Breast Imaging Reporting and Data System 5th edition criteria. Among 38 enrolled patients (mean age, 45±11.45 years; range, 26-75 years; median, 44 years), 63.2% presented with a breast lump and 26.3% underwent screening. Histopathology confirmed malignancy in 26 cases (68.4%), comprising 12 cases of ductal carcinoma *in situ* and 14 of invasive ductal carcinoma. Segmental enhancement was the most common malignant pattern [positive predictive value (PPV), 83.3%], followed by regional enhancement (PPV, 64.3%). Benign lesions had slow (58.3%) or medium (41.7%) initial upslopes, whereas 50% of malignant tumors exhibited a rapid initial slope ($P=0.001$). Persistent delay was observed in 75% of benign cases but in only 26.9% of malignant cases ($P=0.005$). Integrating the initial upslope with the plateau-phase kinetics increased the PPV for malignancy from 75 to 81.8%. In conclusion, the integration of initial-phase

kinetics with traditional delayed-phase and morphological assessment improves the diagnostic accuracy for malignant NME lesions. This multi-parametric approach could potentially serve as a valuable tool to reduce the rate of unnecessary biopsies in the future.

Introduction

Breast cancer remains a notable global health concern. In 2022, it was the most frequently diagnosed cancer among women worldwide, with ~2.3 million novel cases and 666,000 associated mortalities (1). The early diagnosis of breast cancer is of notable importance, as it can increase the 5-year survival rate to 96% (2). Breast magnetic resonance imaging (MRI) demonstrates markedly increased efficacy in detecting lesions in women who possess either a markedly elevated risk of breast cancer or an average risk with dense breast tissue (3). Furthermore, the utilization of breast MRI offers advantages in a variety of additional clinical scenarios, such as the evaluation of tumor extent (3). A common finding in dynamic contrast-enhanced breast MRI (DCE-MRI) is non-mass enhancement (NME). It refers to an enhancing abnormality that is separate from background parenchymal enhancement but lacks the 3-dimensional volume, shape or margin characteristics to be described as a mass.

The approach to NME presents notable challenges due to the considerable overlap in imaging characteristics of benign and malignant etiologies (4). A recent study reported that 51.5% of NME cases were benign and 48.5% were malignant (5). The morphological evaluation of NME comprises two components. The first component pertains to the distribution, which may be classified as linear, focal, segmental, regional, involving multiple regions or diffuse. The second component involves the internal enhancing patterns, which can be categorized as homogeneous, heterogeneous, clustered ring or clumped (6). The dynamics of contrast enhancement serves as a key secondary diagnostic tool (7). The initial increase typically indicates the extent of tumor angiogenesis, while the subsequent 'delay' phase is indicative of the development of stromal tumor cells (7). Early enhancement occurs within 2 min of agent injection. During this time, the initial rise of the enhanced curve can be divided into three categories: 'Slow', 'medium' and 'rapid'. Rapid enhancement is defined as an initial peak signal intensity (SI) >90% within 90 sec, which is a

Correspondence to: Dr Areege Mustafa Kamal, Department of Pathology, Oncology Teaching Hospital, Medical City, 17 Bab Al-Moadam Road, Baghdad 89WH+9MF, Iraq
E-mail: areegekamal@gmail.com

Key words: contrast-enhanced breast MRI, non-mass enhancement, dynamic curve, initial phase

strong indicator of malignancy (6,7). The 'delayed phase' refers to the SI of 2 min post-contrast injection. Based on the delayed phase, kinetic curves are categorized as persistent enhancement (Type I), plateau (Type II) or washout (Type III) (6).

While the diagnostic value of the delayed phase in NME has been extensively studied (8-11), the value of initial phase in such lesions is not generally recognized. Therefore, the present study aimed to investigate the combined use of initial- and delayed-phase kinetics and morphological features to improve the differentiation between benign and malignant NME lesions.

Patients and methods

Study design and population. The present study was a prospective study conducted in the Oncology Teaching Hospital, Medical City (Baghdad, Iraq) from April 2022 to December 2022. The study protocol was approved by the Ethics Committee of the Institutional Review Board at the College of Medicine, University of Baghdad (approval no. 1458; Baghdad, Iraq).

Inclusion criteria were as follows: i) Consecutive female patients referred for breast MRI, either for screening purposes or for further characterization of a previously identified lesion; ii) presence of a pure non-mass enhancement (NME) lesion on MRI; iii) absence of any associated mass or focal mass-like enhancement and iv) available image-guided core biopsy for histopathological evaluation. Excisional biopsy was performed when indicated by core biopsy findings or at the discretion of the treating physician.

Exclusion criteria: 1- Patients without a definitive histopathological diagnosis (e.g., biopsy not performed, inadequate tissue sample). 2- Cases with borderline findings on core biopsy (such as atypical ductal hyperplasia, lobular neoplasia, or other indeterminate lesions) were excluded if no subsequent surgical pathology report was available. 3- Patients lacking sufficient demographic or clinical information in medical records were excluded from final analysis.

Histopathological diagnoses were classified according to the World Health Organization (WHO) Classification of Breast Tumours, 5th Edition (2019) (12).

Image analysis. For each area of NME the data collected are according to the features mentioned in the 5th edition of Breast Imaging Reporting and Data System (BI-RADS) 2013 (12).

Initially, subtracted images were reviewed to identify the NME lesion and evaluate its morphological features, including maximal size, distribution (focal, linear, segmental, regional or diffuse) and internal enhancement pattern (homogeneous, heterogeneous, clumped or clustered ring) and the dynamic curve. For dynamic curve, two components were assessed: i) The initial phase representing the SI observed within the first 2 min, divided into 3 groups as per American College of Radiology BI-RADS 5th edition: Slow, when <50% increase in SI, medium, when 50-100% increase in SI and rapid, when >100% increase in SI occurs within the first 2 min; and ii) the delayed phase represents the enhancement pattern after 2 min or when the curve starts to change. It is grouped as: Persistent, when there is continuous signal increase >10% over time, plateau, when SI does not change over time after its initial rise and remains flat, and washout, when SI decreases >10% after

its highest point from its initial rise indicating a suspicious finding.

MRI imaging protocol. A superconducting 1.5T MR imaging device (Magnetom Aera; Siemens Healthineers) was used for the breast MRI. All patients were examined in the prone position by applying bilateral 16-channel breast coils and using scout view sagittal protocol localization and T1-weighted pulses.

Fast spin-echo was utilized to collect axial non-fat saturated T1-weighted imaging (T1WI) with the following image parameters: i) Repetition time (TR), 426 msec; ii) echo time (TE), 4.6 msec; iii) slice thickness, 4 mm; iv) field of view (FOV), 380x380 mm; and v) matrix, 307x512. The settings for axial non-fat-suppressed T2-weighted turbo spin-echo were TR, 6,030 msec; TE, 71 msec; FOV, 400x400 mm; matrix, 384x512; and 4 mm slice thickness.

To get axial short T2 Transverse Dixon fat and water, the settings were TR, 9,440 msec; TE, 72 msec; slice thickness, 3 mm; inter-slice gap, 1 mm; FOV, 450x450 mm and matrix, 307x512.

Dynamic contrast study was performed by applying fluorescence-3D T1WI spectral attenuated inversion recovery sequence with injection of a 0.2 mmol/kg gadopentetate dimeglumine bolus by an automated injector at 3-5 ml/sec via an 18-20 gauge IV cannula in the antecubital vein. The parameters applied were: i) TR, 5.08 msec; ii) TE, 2.39 msec; iii) 1.8 mm slice thickness; iv) no inter-slice gap; v) FOV, 360x360 mm; and vi) matrix, 307x512. Next, a 20 ml saline bolus infusion at 3-5 ml/sec was administered.

The dynamic series consisted of one pre-contrast and five post-contrast acquisitions; each repeated every 90 sec.

DCE-MRI analysis. Initially, the subtracted images of each examination were evaluated by RadiAnt DICOM viewer 2022.2 (Medixant) to detect the NME lesion and assess its size, distribution and the internal enhancement pattern. Subsequently, the non-subtracted images with pre-contrast T1W image and the four post-contrast images were evaluated. A region of interest was manually placed on the area of highest enhancement within the NME on the first post-contrast series, then time-intensity plots of dynamic images were generated using computer-assisted diagnosis software.

The percentage of the initial enhancement was calculated as follows: $(SI_{post} - SI_{pre}/SI_{pre}) \times 100$, where SI_{pre} and SI_{post} are the SIs on the pre- and first post-contrast images, respectively (13).

Statistical analysis. The SPSS software for windows (version 26; IBM Corp.) was used for all statistical analyses. Observational data was presented in the form of frequencies and percentages. Associations between categorical variables were assessed using the χ^2 or Fisher's exact test, as appropriate. To estimate malignancy likelihood for lesions exhibiting a specific enhancement pattern (Type I with initial rise), the positive predictive value (PPV) was calculated as the proportion of test-positive cases that were confirmed malignant. As sensitivity and specificity assess overall MRI performance and not sub-classification, applying them to Type I curves, typically benign, can misrepresent diagnostic value. PPV further captures the significance of atypical malignant presentations

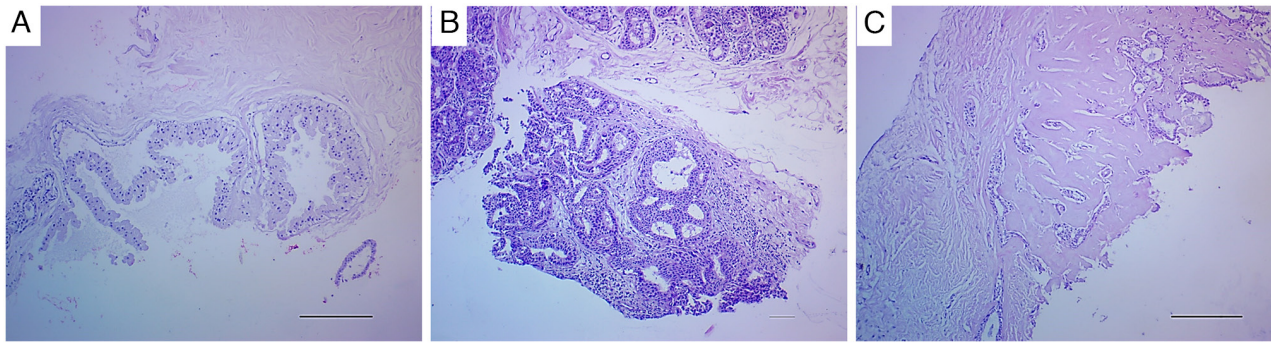


Figure 1. Representative histology of breast lesions associated with dynamic curve types: (A) Fibrocystic changes associated with Type I curve with an initial medium rise (50-100%), (B) extensive intermediate grade ductal carcinoma *in situ* associated with Type I curve with an initial medium rise (50-100%) and (C) invasive ductal carcinoma associated with Type III curve with rapid initial rise (>100%). Hematoxylin and eosin staining; magnification, x100, scale bar is 200 μm .

within this curve type. It reflects real-world decision-making more accurately in this context. A two-sided $P < 0.05$ was considered to indicate a statistically significant difference.

Results

Patient characteristics. A total of 38 patients met the enrollment criteria; their ages ranged from 26 to 75 years, with a mean age of 45 ± 11.45 years. A total of 12 patients (31.6%) were in the postmenopausal period. The majority of the patients 24 (63.2%), presented with a breast lump, whereas 10 individuals (26.3%) were scheduled for screening. The initial mammography revealed microcalcifications in 12 patients (41.4%) and focal asymmetry in 17 patients (58.6%). Furthermore, 7 patients (18.4%) were referred for further imaging due to the presence of dense breast tissue. The definitive histopathological diagnosis was corroborated through core biopsy in 6 cases (15.8%) and via surgical excision in 32 cases (84.2%). Histopathological evaluation confirmed the presence of malignancy in 26 cases, representing 68.4% of the total, while the remaining 12 cases, accounting for 31.6%, were classified as benign (Fig. 1). Half of the benign lesions were inflammatory (acute and granulomatous mastitis), 4 (33.3%) exhibited fibrocystic changes (Fig. 1A), one of which exhibited atypical ductal hyperplasia and the remaining 2 (16.7%) were benign intraductal papilloma. Among the malignant lesions examined, 12 (46.2%) were classified as ductal carcinoma *in situ* (DCIS; Fig. 1B), while invasive ductal carcinoma (IDC) accounted for 14 (53.8%; Fig. 1C). Details are presented in Table I.

MRI features of NME lesions and final histopathology diagnosis. The homogeneous pattern of NME was significantly more frequent in benign lesions (8/12; 66.7%) compared with that in malignant lesions (8/26, 30.8%) ($P = 0.038$). By contrast, heterogenous and clumped patterns were more frequently observed in malignant tumors 10 (38.5%) and 7 (26.9%), respectively compared with 2 (16.7%) of benign lesions, although the difference was not significant ($P > 0.05$; Table II). There was no significant difference between benign and malignant tumors in terms of the enhancement distribution ($P > 0.05$); however, segmental enhancement was the most frequent enhancement encountered in malignant lesion 10 (38.5%) with a PPV of 83.3% compared with 2 (16.7%) of the

Table I. Patient characteristics.

Characteristic	n	Percentage (%)
Age, years		
<40	17	44.7
≥ 40	21	55.3
Menopausal status		
Premenopausal	26	68.4
Postmenopausal	12	31.6
Presentation		
Screening	10	26.3
Lump	24	63.2
Nipple discharge	4	10.5
Mammography		
Asymmetry	17	58.6
Microcalcification	12	41.4
Dense breast	7	18.4
Type of biopsy		
Core needle	6	15.8
Surgical excision	32	84.2
Histopathology		
Benign	12	31.6
Inflammation	6	50.0
Fibrocystic changes	3	25.0
Fibrocystic with atypical ductal hyperplasia	1	8.3
Intraductal papilloma	2	16.7
Malignant	26	68.4
Ductal carcinoma <i>in situ</i>	12	46.2
Invasive ductal carcinoma	14	53.8

benign lesions followed by the regional type 9 (34.6%) with a PPV of 64.3%. When comparing invasive and *in situ* carcinomas, regional enhancement was significantly associated with IDC, occurring in 8 (57.1%) of IDC cases vs. 1 (8.3%) of DCIS cases ($P = 0.014$). The dynamic curve of malignant lesions was significantly different compared with that of

Table II. MRI of the non-mass enhancement lesions and final histopathological outcome.

A, Enhancement							
Parameter	Malignant, n (%)	Benign, n (%)	P-value	PPV, %	DCIS, n (%)	IDC, n (%)	P-value
Homogenous	8.0 (30.8)	8.0 (66.6)	0.037 ^a	50.0	5.0 (41.7)	3.0 (21.4)	0.401
Heterogenous	10.0 (38.5)	2.0 (16.7)	0.268	83.4	3.0 (25)	7.0 (50)	0.248
Clumped	7.0 (26.9)	2.0 (16.7)	0.689	77.8	3.0 (25)	4.0 (28.6)	>0.999
Cluster ring	1.0 (3.80)	0.0 (0.0)	>0.999	100.0	1.0 (8.3)	0.0	0.462
B, Distribution							
Parameter	Malignant, n (%)	Benign, n (%)	P-value	PPV, %	DCIS, n (%)	IDC, n (%)	P-value
Focal	3.0 (11.5)	2.0 (16.7)	0.643	60.0	3.0 (25.0)	0.0	0.085
Linear	1.0 (3.9)	2.0 (16.7)	0.229	33.3	1.0 (8.3)	0.0	0.462
Segmental	10.0 (38.5)	2.0 (16.7)	0.268	83.3	5.0 (41.7)	5.0 (35.7)	>0.999
Regional	9.0 (34.6)	5.0 (41.6)	0.675	64.3	1.0 (8.3)	8.0 (57.1)	0.014 ^a
Diffuse	3.0 (11.5)	1.0 (8.3)	>0.999	75.0	2.0 (16.7)	1.0 (7.1)	0.580

^aP<0.05. PPV, positive predictive value; DCIS, ductal carcinoma *in situ*; IDC, invasive ductal carcinoma; MRI, magnetic resonance imaging.

Table III. MRI dynamic curve of non-mass enhancement lesions and final histopathological outcome.

Parameter	Malignant, n (%)	Benign, n (%)	P-value	PPV, %
Initial upslope			0.001 ^a	
Slow, <50%	3.0 (11.5)	7.0 (58.3)		30.0
Medium, 50-100%	10.0 (38.5)	5.0 (41.7)		66.7
Rapid, >100%	13.0 (50.0)	0.0		100.0
Delay phase			0.005 ^a	
Type I	7.0 (26.9)	9.0 (75.0)		46.8
Type II	9.0 (34.6)	3.0 (25.0)		75.0
Type III	10.0 (38.5)	0.0		100.0

^aP<0.05. PPV, positive predictive value; MRI, magnetic resonance imaging; Type I, persistent; Type II, plateau; Type III, washout.

the benign ones in terms of initial upslope and delay phase, P=0.001 (Table III; Figs. 2-4). Benign lesions exhibited slow initial upslope in 7 (58.3%) of the cases while five (41.7%) have medium initial slope. By contrast, rapid initial slope was the feature of 13 (50%) of malignant tumors (P=0.001; Fig. 3). A persistent delay phase was the significant feature of 9 (75%) of the benign lesions compared with only 7 (26.9%) malignant lesions (P=0.005; Fig. 2). None of the benign lesions exhibited rapid initial or washout delay phase.

To further evaluate the 16 cases with persistent delay phase, kinetic analysis of the initial phase was performed. Among the benign lesions, a slow initial phase was observed in 6 cases (66.7%), while 3 (33.3%) exhibited medium initial phase. However, a slow initial phase was also observed in 3 (42.9%) and a medium in 4 (57.1%) of the malignant lesions (P=0.615) (Table IV; Fig. 2C and D). Among the 12 lesions with a plateau delayed phase, 1 out of the 3 benign lesions exhibited slow initial phase (Fig. 3A and B; however, none of the malignant

lesions depicted slow initial phase, yet the difference was not significant (P=0.159; Table IV).

Combining initial phase to delay phase curve enhances the PPV. As illustrated in Table V, the PPV of the persistent curve is relatively notably high at 43.8%. However, the PPV was diminished by ~10% (33.3%) upon the inclusion of the initial phase upslope of <50%. By contrast, adding initial upslope >50% to plateau curve increased the PPV from 75 to 81.8%. Although the plateau curve achieved 100% PPV enhanced with the addition of initial upslope >100% (Table V), the detection rate was 5 of 9 malignant cases confirmed by histopathology in this category (Table III).

Discussion

In the present study, the MRI features of NME lesions were evaluated with a particular focus on the initial and delayed

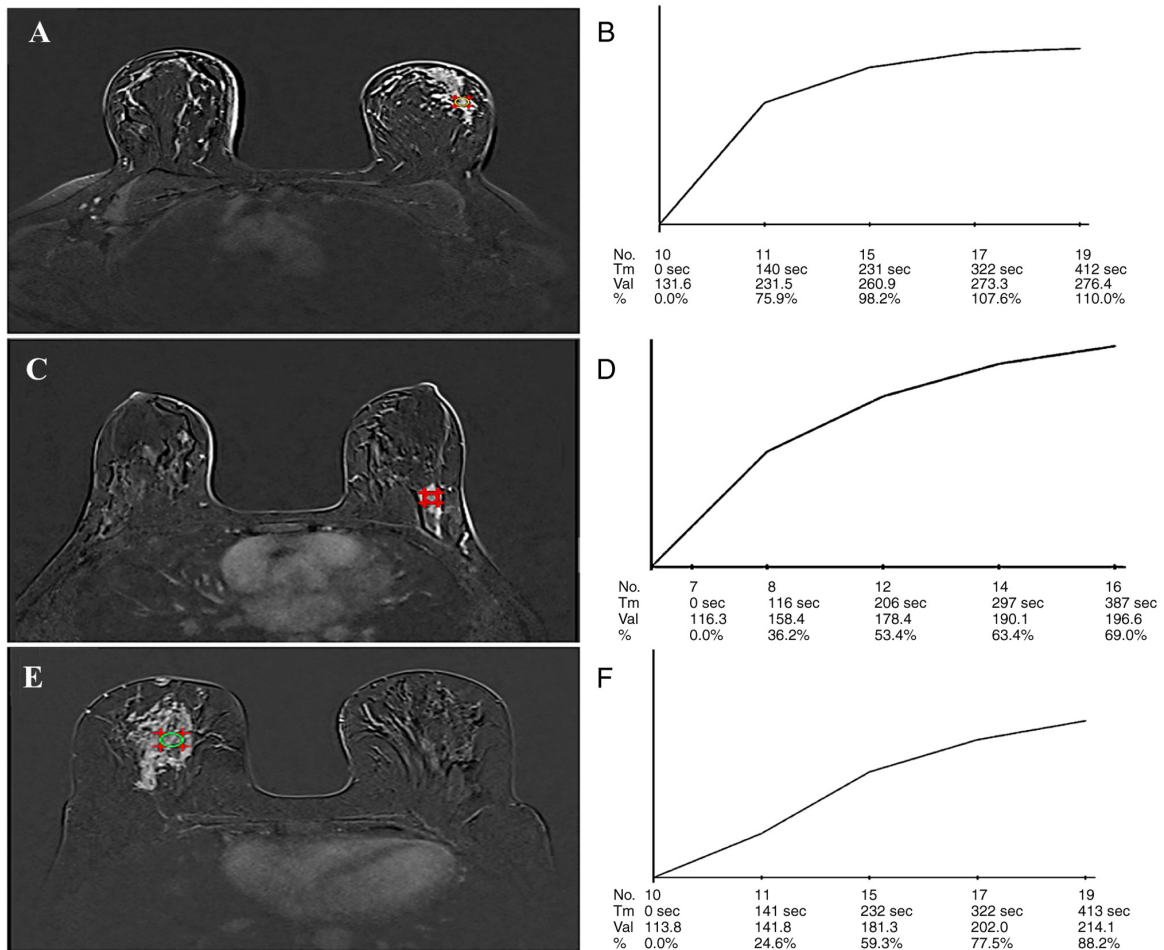


Figure 2. Dynamic contrast study of three women with histopathology-confirmed ductal carcinoma *in situ*, demonstrating a Type I curve with varying initial phases. (A) A 50-year-old woman with a palpable left breast lesion. MRI shows non-mass enhancement with green and red labels representing the region of interest (ROI), (B) Time intensity curve exhibited a Type I curve with an initial moderate rise (50-100%). (C) A 45-year-old woman with a palpable left lump, MRI shows non-mass enhancement with red label representing the region of interest (ROI). (D) Time intensity curve exhibited a Type I curve with a slow initial rise (<50%). (E) A 65-year-old woman with a palpable right lump. (F) Time intensity curve exhibited a Type I curve with a slow initial rise (<50%). Type I, persistent.

Table IV. Initial upslope stratified in Type I and II curve and final histopathological outcome.

Parameter	Malignant, n (%)	Benign, n (%)	P-value
Type I cases (n=16)			0.615
Slow, <50%	3.0 (42.9)	6.0 (66.7)	
Medium, 50-100%	4.0 (57.1)	3.0 (33.3)	
Rapid, >100%	0.0	0.0	
Type II cases (n=12)			0.159
Slow, <50% initial	0.0	1.0 (33.3)	
Medium, 50-100% initial	4.0 (44.4)	2.0 (66.7)	
Rapid, >100% initial	5.0 (55.6)	0.0	

Type I, persistent; type II, plateau.

Table V. PPV of dynamic curve and with and without including the initial curve slope cut-off 50 and 100%.

Phase	MRI dynamic	Total no.	PPV, %
Delay	Type I	16	43.8
	Type II	12	75.0
	Type III	10	100.0
Initial, %	<50	10	30.0
	50-100	15	66.7
	>100	13	100.0
Combined	Type I and <50% initial	9	33.3
	Type II and >50% initial	11	81.8
	Type II and >100% initial	5	100.0

PPV, positive predictive value; Type I, persistent; Type II, plateau; Type III, washout.

phases of the DCE kinetic curve. Although previous research has extensively explored the role of enhancement patterns and distribution in predicting malignancy (8-11), integrated

analysis of early and delayed kinetic phases remains inadequately investigated. Of 38 NME lesions, malignancy was

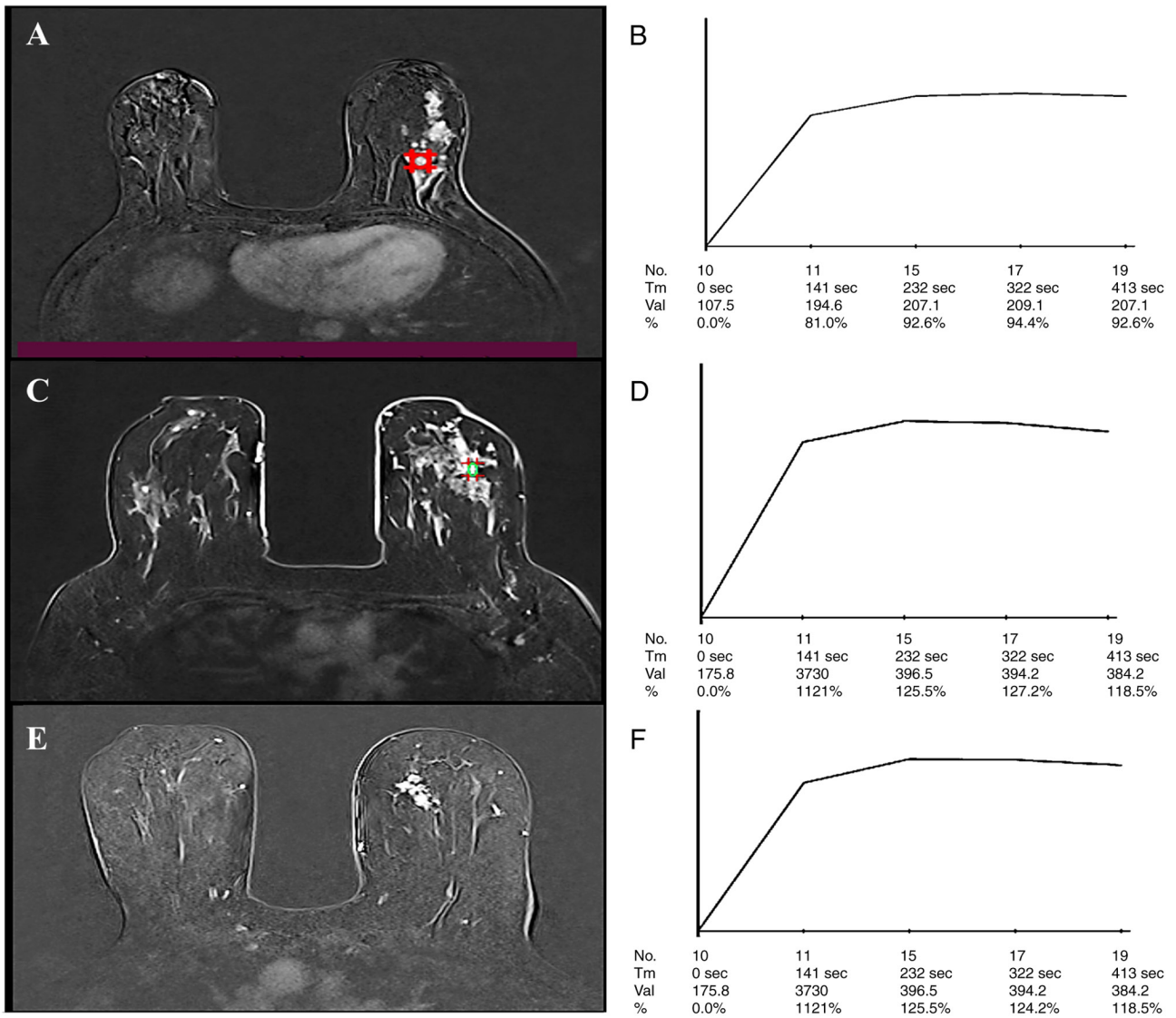


Figure 3. Dynamic contrast study of three women exhibiting a Type II curve with different initial phases. (A) A 27-year-old woman with a palpable left lump, MRI shows non-mass enhancement with red label representing the region of interest. (B) Time intensity curve displayed a Type II curve with an initial moderate rise (50-100%). Histopathology confirmed granulomatous mastitis. (C) A 36-year-old woman with a left breast lump, MRI shows non-mass enhancement with green and red labels representing the region of interest (ROI). (D) Time intensity curve exhibited a Type II curve with a rapid initial rise (>100%), diagnosed as DCIS on excision. (E) A 75-year-old woman with a left breast lump, MRI shows non-mass enhancement. (F) Time intensity curve demonstrated a Type II curve with an initial moderate rise (50-100%), confirmed as DCIS upon excision. DCIS, ductal carcinoma *in situ*; Type II, plateau.

verified in 26 (68.4%), with nearly half (46.2%) classified as *in situ* tumors. Segmental enhancement distribution was the main finding of malignant tumors, which accounted for 10 cases (38.5%) with a PPV of 83.3% consistent with previous studies reporting PPV values ranging from 67 to 100% (10,14).

The regional distribution was the predominant pattern overall (14/38, 36.8% of NME lesions) and ranked second among malignancies (34.6%). Notably, this distribution was significantly associated with IDCs, occurring in 57.1% of IDCs vs. only 8.3% of DCIS cases.

DCIS-associated NME typically exhibited segmental or linear patterns, reflecting ductal system involvement, often with clumped or heterogeneous enhancement (15). Consistent with this finding, segmental distribution was the most frequent feature of DCIS lesion in the present study, 5 (41.7%), followed by focal 3 (25%). Homogeneous enhancement was significantly more common in benign lesions (66.7% vs. 30.8% in malignancies).

Nonetheless, 41.7% of DCIS cases also displayed homogeneous enhancement, highlighting the overlap between low/intermediate-grade DCIS and benign lesions. This aligns with the study by Yoon *et al* (15), which reported homogeneous enhancement in 33.3% of DCIS cases.

Both the initial and delayed kinetic phases exhibited significant disparities between malignant and benign lesions. Malignancies predominantly exhibited a Type III (washout) curve, whereas benign lesions typically demonstrated a Type I (persistent) curve, consistent with findings by Yang *et al* (8), Liu *et al* (9) and Aydin (10).

The washout curve attained 100% PPV while the plateau curve reached 75%. Bluemke *et al* (16) reported that plateau and washout patterns were 63.2% sensitive and 65.4% specific for malignancy (16). However, the interpretation of Type II (plateau) curves remains controversial. Although certain studies associate them with malignancy, Zhou *et al* (11)

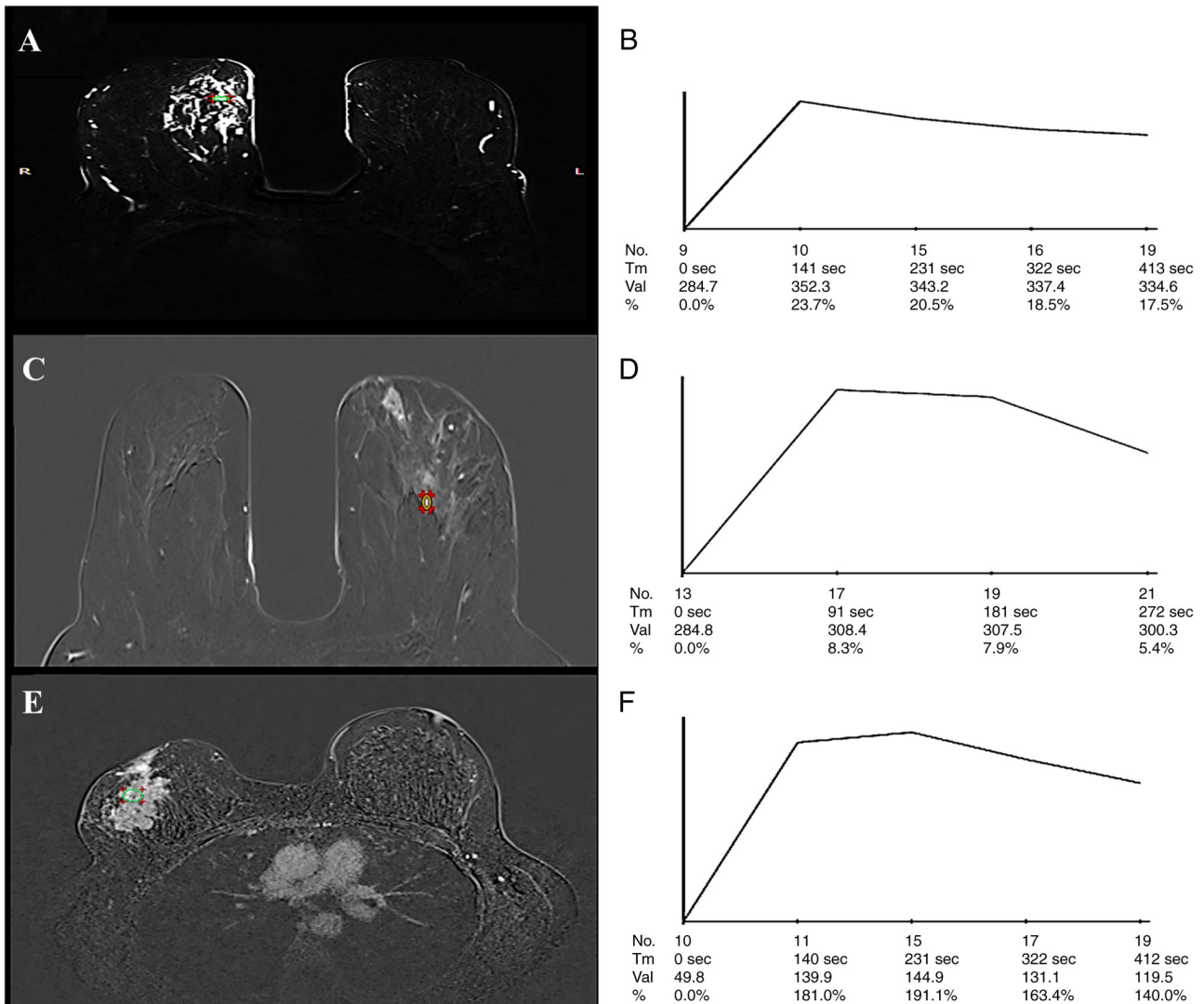


Figure 4. Dynamic contrast study of three women exhibiting a Type III curve with different initial phases. (A) A 57-year-old woman with a right breast lump, MRI shows non-mass enhancement with green label representing the region of interest (ROI), (B) Time intensity curve demonstrated a Type III curve with a rapid initial rise (>100%). Histopathology confirmed DCIS with invasive ductal carcinoma. (C) A 50-year-old woman with a palpable breast lump. MRI shows non-mass enhancement with red labels representing the region of interest (ROI), (D) Time intensity curve exhibited a Type III curve with a rapid initial rise (>100%), diagnosed as DCIS without invasive components on excision. (E) A 36-year-old woman with a right breast lump. (F) Time intensity curve exhibited a Type III curve with a rapid initial rise (>100%). Core biopsy revealed invasive ductal carcinoma. DCIS, ductal carcinoma *in situ*; Type III, washout.

reported that Type II curves in NME were more frequent in benign papillary neoplasms; the present study data suggested that integrating the initial upslope magnitude can refine diagnostic accuracy. The present study identified that combining type I curve with slow initial phase (<50%) reduced the PPV by ~10% while combining type II curve with initial >50% increased the PPV from 75 to 81.8%. A Type II curve with an initial upslope >100% achieved 100% PPV; however, this resulted in diminished sensitivity. These findings suggest that incorporating the initial upslope could enhance malignancy prediction in NME lesions. However, larger studies are warranted to validate these observations and assess their clinical utility in the future.

The main limitation of the present study was the limited number of enrolled cases and the loss of cases during follow-up. As a single-center, proof-of-concept study, the primary aim was not to provide final validation but to identify and define promising MRI criteria (such as the combined 'II

and >100% initial' feature) under controlled, expert conditions. A multi-center validation is warranted to assess the generalizability of these criteria across radiologists of diverse experience levels and MRI platforms. Furthermore, the present study results provided key preliminary data necessary to power future studies. Based on the observed effect sizes in the present study (for example, ~100 vs. ~33% PPV between groups), a sample size calculation for a future validation study can be performed.

In conclusion, integration of initial upslope kinetics alongside conventional delayed-phase analysis and morphological features (for example, distribution and internal enhancement) may improve diagnostic accuracy for malignant NME lesions, potentially reducing unnecessary biopsies in the future.

Acknowledgements

Not applicable.

Funding

No funding was received.

Availability of data and materials

The data generated in the present study may be requested from the corresponding author.

Authors' contributions

TFK conceived the research idea for the present study. TFK and MAN planned the present study and collected the cases. AMK analyzed the data and drafted the manuscript. TFK conceptualized and designed the present study, performed the literature search, identified clinical studies, conducted the data and statistical analysis, prepared and reviewed the manuscript. AMK conceptualized and designed the present study, conducted the data analysis, prepared and reviewed the manuscript. MAN prepared and reviewed the manuscript. TFK and AMK confirm the authenticity of all the raw data. All authors reviewed and edited the manuscript. All authors read and approved the final version of the manuscript.

Ethics approval and consent to participate

The Ethics Committee of the Institutional Review Board at the College of Medicine, University of Baghdad, provided approval for the present study (approval no. 1458; Baghdad, Iraq). Written informed consent was obtained from each patient for participation in the present study and for the use of their samples in scientific research, in accordance with the Declaration of Helsinki.

Patient consent for publication

A statement of consent for publication was signed by each patient according to the principles of the Declaration of Helsinki.

Competing interests

The authors declare that they have no competing interests.

Authors' information

ORCID: AK, 0000-0001-5239-9699.

References

- Bray F, Laversanne M, Sung H, Ferlay J, Siegel RL, Soerjomataram I and Jemal A: Global cancer statistics 2022: GLOBOCAN estimates of incidence and mortality worldwide for 36 cancers in 185 countries. *CA Cancer J Clin* 74: 229-263, 2024.
- Sree SV, Ng EY, Acharya RU and Faust O: Breast imaging: A survey. *World J Clin Oncol* 2: 171-178, 2011.
- Wekking D, Porcu M, De Silva P, Saba L, Scartozzi M and Solinas C: Breast MRI: clinical indications, recommendations, and future applications in breast cancer diagnosis. *Curr Oncol Rep* 25: 257-267, 2023.
- Gargiulo M, Dien E, Gal J, Schiappa R, Elkind L and Lamarque M: Predictive factors for non-mass enhancement occult in conventional breast imaging: The 'PAMAS' study. *Eur J Radiol* 184: 111962, 2025.
- Mohamed S, Elhamd EA and Attia NM: Non-mass enhancement on breast MRI: Clues to a more confident diagnosis. *Egypt J Radiol Nucl Med* 55: 87, 2024.
- Spak DA, Plaxco JS, Santiago L, Dryden MJ and Dogan BE: BI-RADS® fifth edition: A summary of changes. *Diagn Interv Imaging* 98: 179-190, 2017.
- Cheng L, Bai Y, Zhang J, Liu M, Li X, Zhang A, Zhang X and Ma L: Optimization of apparent diffusion coefficient measured by diffusion-weighted MRI for diagnosis of breast lesions presenting as mass and non-mass-like enhancement. *Tumour Biol* 34: 1537-1545, 2013.
- Yang QX, Ji X, Feng LL, Zheng L, Zhou XQ, Wu Q and Chen X: Significant MRI indicators of malignancy for breast non-mass enhancement. *J Xray Sci Technol* 25: 1033-1044, 2017.
- Liu G, Li Y, Chen SL and Chen Q: Non-mass enhancement breast lesions: MRI findings and associations with malignancy. *Ann Transl Med* 10: 357, 2022.
- Aydin H: The MRI characteristics of non-mass enhancement lesions of the breast: Associations with malignancy. *Br J Radiol* 92: 20180464, 2019.
- Zhou J, Li M, Liu D, Sheng F and Cai J: Differential diagnosis of benign and malignant breast papillary neoplasms on MRI with non-mass enhancement. *Acad Radiol* 30 (Suppl 2): S127-S32, 2023.
- D'Orsi C, Sickles E and Mendelson E and Morris EA: ACR BI-RADS Atlas: Breast Imaging Reporting and Data System. American College of Radiology, Reston, VA, 2013.
- Cheng L and Li X: Breast magnetic resonance imaging: Kinetic curve assessment. *Gland Surg* 2: 50-53, 2013.
- Asada T, Yamada T, Kanemaki Y, Fujiwara K, Okamoto S and Nakajima Y: Grading system to categorize breast MRI using BI-RADS 5th edition: A statistical study of non-mass enhancement descriptors in terms of probability of malignancy. *Jpn J Radiol* 36: 200-208, 2018.
- Yoon GY, Choi WJ, Cha JH, Shin HJ, Chae EY and Kim HH: The role of MRI and clinicopathologic features in predicting the invasive component of biopsy-confirmed ductal carcinoma in situ. *BMC Med Imaging* 20: 95, 2020.
- Bluemke DA, Gatsonis CA, Chen MH, DeAngelis GA, DeBruhl N, Harms S, Heywang-Köbrunner SH, Hylton N, Kuhl CK, Lehman C, *et al*: Magnetic resonance imaging of the breast prior to biopsy. *JAMA* 292: 2735-2742, 2004.



Copyright © 2026 Kareem et al. This work is licensed under a Creative Commons Attribution-NonCommercial-NoDerivatives 4.0 International (CC BY-NC-ND 4.0) License.